

Constructal heat transfer and fluid flow enhancement optimization for cylindrical microcooling channels with variable cross-section

Olabode T. Olakoyejo¹  | Adekunle O. Adelaja¹  |
Olayinka O. Adewumi¹ | Adeyinka A. Oluwo¹ |
Solomon K. Bello² | Saheed A. Adio³ 

¹Department of Mechanical Engineering, University of Lagos, Akoka, Nigeria

²Department of Mechanical Engineering Technology, Lagos State Polytechnic, Ikorodu, Nigeria

³Department of Mechanical Engineering, Obafemi Awolowo University, Ileife, Nigeria

Correspondence

Olabode T. Olakoyejo, Department of Mechanical Engineering, University of Lagos, Akoka, Lagos 100001, Nigeria.
Email: oolakoyejo@unilag.edu.ng

Abstract

This study applies constructal theory to conduct a numerical optimization of three-dimensional cylindrical microcooling channels with the solid structure subjected to internal heat generation. The cylindrical channels are designed as variable cross-section configurations that experience conjugate heat transfer and fluid flow, where water is used as the coolant. The research aims to optimize the channel configurations subject to a fixed global solid material volume constraint. The key objectives are to minimize the global thermal resistance and friction factor. The coolant is pushed through the channels by pressure drop represented as Bejan number. The main design parameters are the inlet and outlet diameters at a given porosity. The channel configuration and the structure elemental volume are permitted to change to find the best design parameters that minimized thermal resistance and friction factor, so that the cooling effect is enhanced. An ANSYS FLUENT code is used to obtain the best optimal parameter of the configuration that enhances thermal performance. The influence of Bejan number on optimized inlet and outlet diameters led to

minimization of thermal resistance and friction factor and maximization of Nusselt number. The results show distinctive optimal inlet and outlet diameters that enhance the overall performance of the system in the range of $1.018 \times 10^{-2} \leq (d_{\text{in}}/L)_{\text{opt}} \leq 1.5381 \times 10^{-2}$ and $1.0838 \times 10^{-2} \leq (d_{\text{out}}/L)_{\text{opt}} \leq 1.6134 \times 10^{-2}$, respectively.

KEYWORDS

Bejan number, constructal theory, maximized Nusselt number, minimized friction factor, minimized thermal resistance, optimization

1 | INTRODUCTION

High-power electronic equipment and heat exchangers are heat-generating devices commonly used in power, air-conditioning, process engineering, electronic, automobile, aerospace, and atomic energy industries. Overheating and thermal stresses always occur due to heat generation in these devices, which causes the failure of the system due to the exceeded temperature limit specified by the manufacturers.

Therefore, there is a need to optimally design this heat-generating device in such a way that the structural geometry is optimized to ensure that the specified temperature limit is maintained. For instance, when designing an array of electronic chips, it is required to arrange the electronic chips into a fixed volume surface or set an array of cooling channels into a specified volume without surpassing the specified temperature threshold. This enhances system thermal performance.

Constructal theory and design^{1–11} is an evolutionary design method for the flow architecture and thermal performance of the cooling channels. This design philosophy is centered on the principle of objectives and constraints that can be used in searching for the configuration of the cooling channel arrangements that will offer the least flow resistance and enhanced system performance. This method has been summarized and put as a constructal law.^{1,2}

Constructal design has been used in biological sciences, social organizations, physics, and engineering for the design of flow systems.^{12–27} For example, in engineering problems, configuration dimension is not known in advance before the optimization begins. It has to be determined optimally, so that the system performance is enhanced.

Bejan and Sciubba²⁰ started applying this theory and method of asymptotes to optimizing the space between parallel plates and channels that enhance the thermal performance in a volume of heat-generating components. Bello-Ochende and co-authors^{28,29} applied constructal theory to carry out research on the optimization of three-dimensional microchannels with a uniform heat flux. They examined and predicted optimal configurations of the cooling channels. The studies were later extended and optimized by inserting pin fins in the microchannel heat sink while the length of the channel was unfixed.³⁰

2 | COMPUTATIONAL MODEL

Figure 1 shows the schematic geometrical configuration under consideration. It is a three-dimensional solid body of a fixed global volume and length (L) experiencing internal heat generation. This structure comprises parallel cylindrical microchannels of variable cross-sectional areas. The structure is cooled by pushing water through channels at different values of Bejan number (Be) to decrease the maximum wall temperature at every hot spot within the volume. The fluid is assumed to be a single-phase, steady, incompressible, and Newtonian with constant properties, negligible viscous dissipation, and radiative heat transfer. The heat distribution inside the structure is symmetrical, and thus helps to save computation time. Figure 2 shows the elemental volume, which consists of a cylindrical cooling channel of a variable

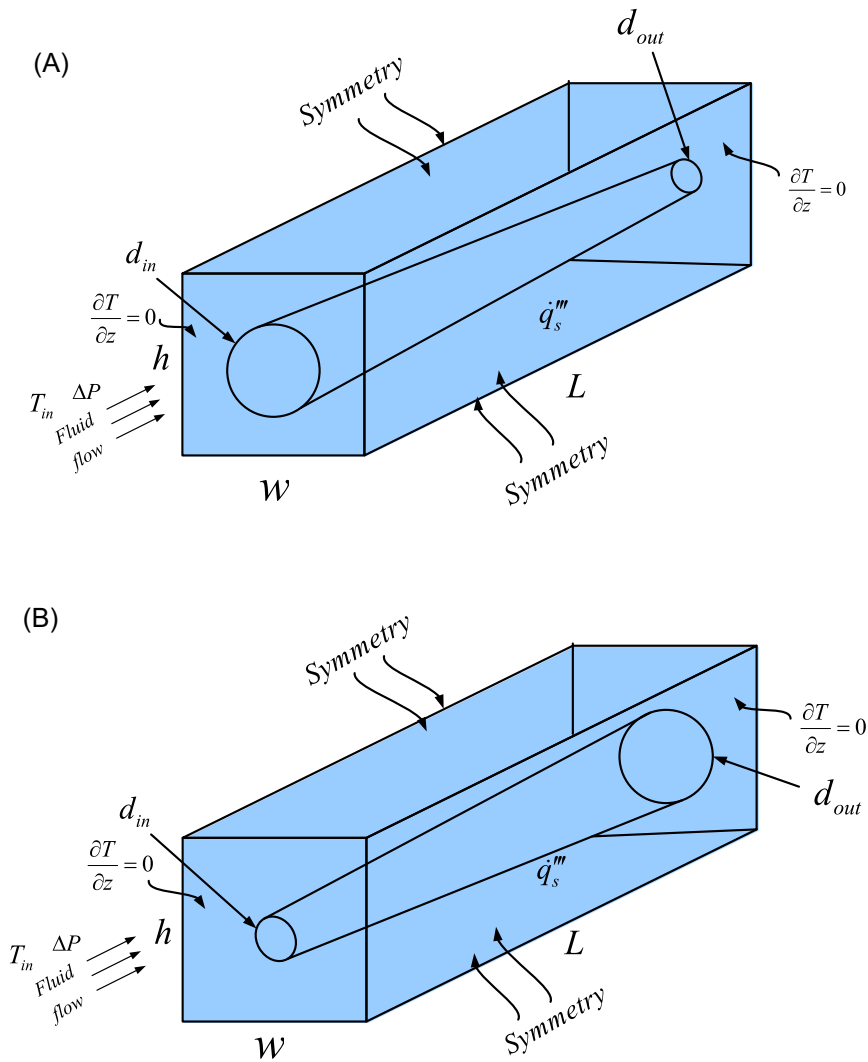


FIGURE 2 Computational domain of the elemental volume with boundary conditions: (A) $d_{in} > d_{out}$ and (B) $d_{in} < d_{out}$ [Color figure can be viewed at wileyonlinelibrary.com]

cross-sectional region and the surrounding solid wall. The elemental cooling channel constraints are considered to be composed of unequal inlet diameter d_{in} and outlet diameter d_{out} . The analysis is a conjugate heat transfer within the entire system.

The porosity of the unit volume of the structure is expressed as follows:

$$\phi = \frac{v_{ch}}{v_{el}} \quad (1)$$

where

$$v_{ch} = \frac{\pi}{12}(d_{in}^2 + d_{in}d_{out} + d_{out}^2)L, d_{in} \neq d_{out} \quad (2)$$

d_{in} and d_{out} are the inlet and outlet diameters of the channel, respectively. v_{el} is the elemental volume of the solid structure, defined as follows:

$$v_{el} = w^2L, w = h, \quad (3)$$

The global volume of the solid body is expressed as follows:

$$V_s = HWL \quad (4)$$

The objective is to determine the best inlet diameter d_{in} and outlet diameter d_{out} that offer the minimum resistance to heat transfer (thermal resistance) and fluid flow (friction factor), thus enhancing the optimal performance of the system.

Figure 3 shows the discretized computational domain of variable cylindrical configuration. The governing equations and boundary conditions used for solving the problem are expressed in Equations (5)–(14) as follows:

$$\nabla \cdot \vec{v} = 0 \quad (5)$$

$$\rho_f(\vec{v} \cdot \nabla \vec{v}) = -\nabla P + \mu_f \nabla^2 \vec{v} \quad (6)$$

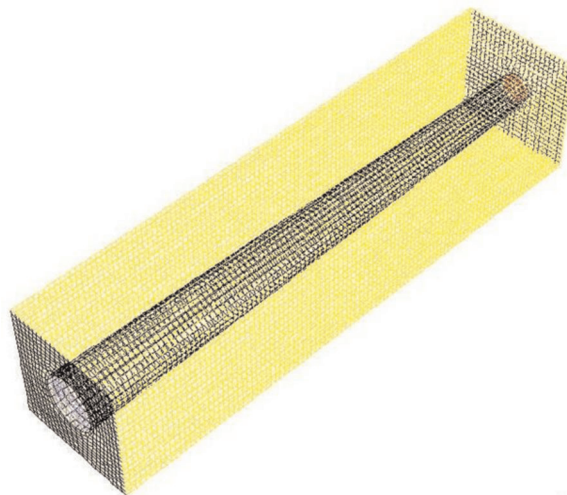


FIGURE 3 Computational domain discretization for a variable cylindrical cooling channel [Color figure can be viewed at wileyonlinelibrary.com]

$$(\rho c_p)_f (\vec{v} \cdot \nabla T) = k_f \nabla^2 T \quad (7)$$

The energy equation for a solid body is given as follows:

$$k_s \nabla^2 T + \dot{q}_s''' = 0 \quad (8)$$

where

$k_s = 148 \text{ W/mK}$ is for silicon material of the solid structure.

The boundary condition at the solid–fluid interface is given as follows:

$$k_s \frac{\partial T}{\partial n} \Big|_s = k_f \frac{\partial T}{\partial n} \Big|_f \quad (9)$$

The channel wall no-slip condition is as follows:

$$\vec{v} = 0 \quad (10)$$

The inlet temperature and pressure boundary conditions are defined in Equations (11) and (12) as follows:

$$T = T_{\text{in}} \quad (11)$$

$$P_{\text{in}} = \frac{Be\alpha\mu}{L^2} + P_{\text{out}} \quad (12)$$

where Be is the Bejan number characterizing the laminar flow in the microchannel.^{41–43}

The outlet temperature and pressure condition are

$$P_{\text{out}} = P_{\text{atm}} \quad (13)$$

The solid body boundaries are expressed as follows:

$$\nabla T = 0 \quad (14)$$

One of the objective functions is the minimum thermal resistance (R_{min}):

$$R_{\text{min}} = \frac{k_f (T_{\text{max}} - T_{\text{in}})_{\text{min}}}{\dot{q}_s''' L^2} \quad (15)$$

It is a function that optimized d_{in} and d_{out} and minimized peak temperature.

3 | NUMERICAL TECHNIQUE

To find the optimal configuration that minimizes the global thermal resistance and friction factor, the channel length, Bejan number, and porosity are fixed. The inlet and outlet diameters with the elemental volume vary with respect to the fixed porosity. The numerical solution for Equations (5)–(14) is achieved using a commercial ANSYS FLUENT code⁴⁴ for the simulation.

The code is based on a finite-volume method that converts the partial differential equations into discrete algebraic equations by the discretization of the computational domain. The technique has been documented in Reference [45]. A second-order upwind scheme is used to discretize the diffusion convection effects in the momentum and energy equations. The SIMPLE algorithm is used to simulate the coupled pressure–velocity fields of the transport equations. The solution converges when the normalized residuals of the continuity and momentum equations fall below 10^{-6} and are lower than 10^{-10} for the energy equation.

4 | GRID INDEPENDENCE TEST AND VALIDATION

Grid independence and sensitivity tests are performed for various elemental volumes and porosities for results accuracy. The convergence criterion for the grid independence is as follows:

$$\gamma = \frac{|(R)_i - (R)_{i-1}|}{|(R)_i|} \leq 0.01 \quad (16)$$

where i and $i - 1$ are the mesh indices for current and previous iterations, respectively. The $i - 1$ mesh is chosen when Equation (16) is fulfilled.

The grid independence test for variable cross-section configuration with $w = h = 4 \times 10^{-4}$ m, $d_{in} = 2 \times 10^{-4}$ m, $d_{out} = 1.5 \times 10^{-4}$ m, $L = 0.01$ m and $Be = 5 \times 10^{10}$ is shown in Table 1. The computational cell density of 288,564 fulfills the convergence criterion; therefore, any increase has a negligible effect on the result.

This current numerical code is compared and validated with a previous research solution of the problem considered and reported by Qu and Mudawar¹⁸ at $q'' = 100$ W/cm² and $200 \leq Re \leq 1600$. Figure 4 shows that the predicted curves have a similar trend with an error margin below 2%.

5 | NUMERICAL RESULTS AND DISCUSSIONS

5.1 | $d_{in} > d_{out}$ Case1 when $d_{in} > d_{out}$ and Case 2 when $d_{in} < d_{out}$

In this section, both cases have the same elemental channel volume and are allowed to vary in the range of 5×10^{-5} m $\leq d_{in} \leq 3 \times 10^{-4}$ m and 5×10^{-5} m $\leq d_{out} \leq 3 \times 10^{-4}$ m. The elemental volume of the structure also changes with respect to the elemental channel volume with fixed porosity $\phi = 0.2$. Also, the axial length of the configuration $L = 0.01$ and applied Bejan number $Be = 5 \times 10^{10}$ are fixed. The internal heat generation is 10^8 W/m³ and the inlet temperature of working fluid is 300K.⁴⁶

Figures 5–8 show the maximum wall temperature against the channel inlet and outlet diameters, channel volume, and elemental volume when $d_{in} > d_{out}$ and $d_{in} < d_{out}$ for prescribed Bejan number and porosity. When the configuration design parameters increase, the peak temperature decreases until it gets to optimal values, and any further increase in design variables increases the peak temperature. At this point, the working fluid has been adequately engaged for the cooling of the solid substrate. The results

TABLE 1 Grid independence study for the variable cross-section cylindrical configuration with $w = h = 4 \times 10^{-4}$ m, $d_{in} = 2 \times 10^{-4}$ m, $d_{out} = 1.5 \times 10^{-4}$ m, $L = 0.01$ m and $Be = 5 \times 10^{10}$

Number of nodes	Number of cells	Number of faces	R	$\gamma = \frac{ (R)_i - (R)_{i-1} }{ (R)_i }$
162,740	136,500	435,280	0.0000658386	–
262,992	230,961	724,406	0.0000703098	0.063593
326,899	288,564	903,463	0.00007083	0.007344
535,664	479,573	1,494,132	0.0000724302	0.022093

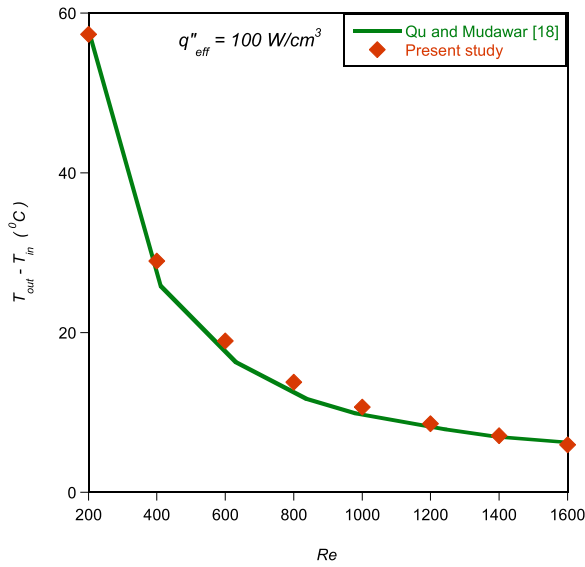


FIGURE 4 Comparison of the present study with Qu and Mudawar¹⁸ [Color figure can be viewed at wileyonlinelibrary.com]

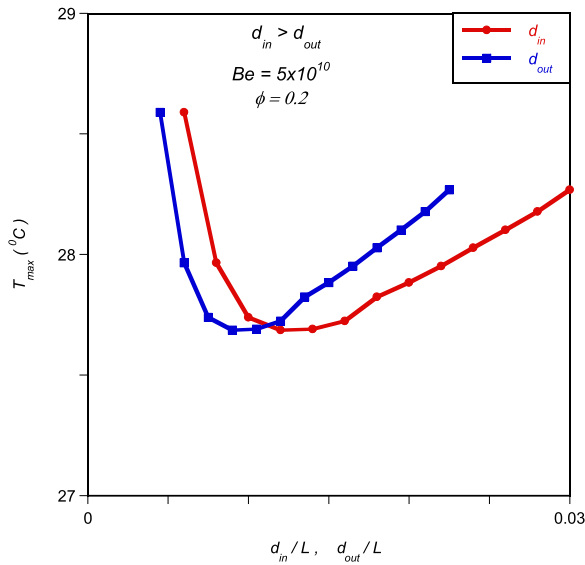


FIGURE 5 Effect of inlet and outlet diameter, $d_{in} > d_{out}$, on the maximum wall temperature [Color figure can be viewed at wileyonlinelibrary.com]

indicate that the optimal configuration arrangements should be very small to maintain enhanced cooling. The curves further reveal that the thermal performance of the microsystem is enhanced when $d_{in} < d_{out}$ for the same channel volume and elemental volume, as can be clearly seen in Figures 7 and 8.

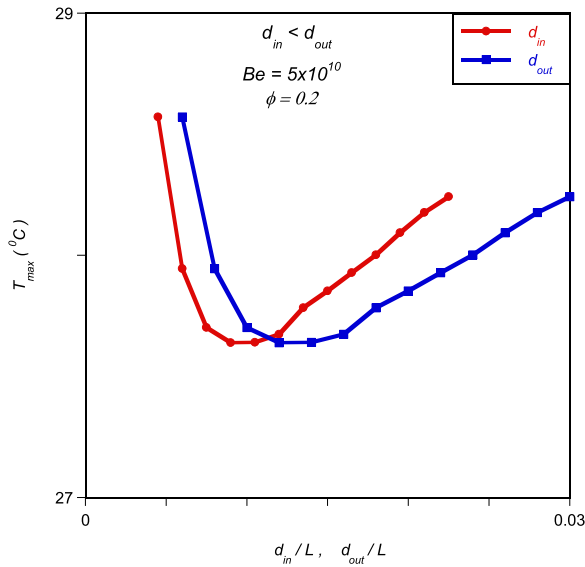


FIGURE 6 Effect of inlet and outlet diameter, $d_{in} < d_{out}$, on the maximum wall temperature [Color figure can be viewed at wileyonlinelibrary.com]

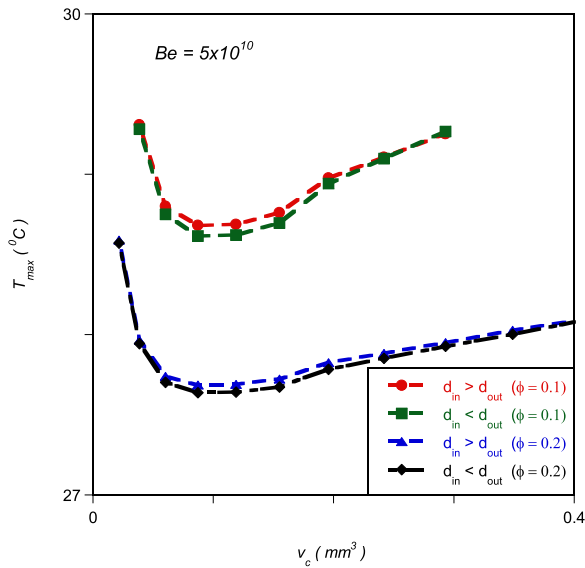


FIGURE 7 Effect of channel volume, v_c , on the maximum wall temperature [Color figure can be viewed at wileyonlinelibrary.com]

5.2 | Response surface optimization

A response surface optimization (RSO) tool whose process is based on the response surface methodology (RSM) is used for the optimization. The details of this method can be found in References [30,47,48]. The RSO is used to find the optimal parameters that make the system perform most efficiently.

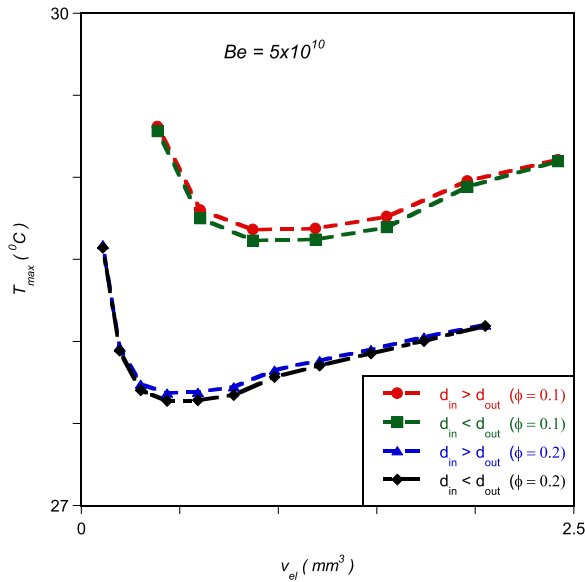


FIGURE 8 Effect of elemental volume, v_{el} , on the maximum wall temperature [Color figure can be viewed at wileyonlinelibrary.com]

To achieve our objective function, a response surface is designed; that is, a number of design of experiments (DOE) are carried out, and in each DOE, the response of interest is measured for specified settings of the design. The optimization then searches for design candidates and later determines the minimized objective functions with the corresponding optimal design variables. Equation (17) shows the design variables ranges for the optimization:

$$5 \times 10^{-5} \text{ m} \leq d_{in} \leq 3 \times 10^{-4} \text{ m}, \quad 5 \times 10^{-5} \text{ m} \leq d_{out} \leq 3 \times 10^{-4} \text{ m}, \quad \phi = 0.1, 0.2, \quad (17)$$

$$h = w = f(d_{in}, d_{out}, \phi), \quad Be = 10^{10} \text{ to } 5 \times 10^{10}$$

Figure 9 presents the graph of minimized, global, dimensionless thermal resistance against the Bejan number and porosity. The result indicates that the minimized thermal resistance decreases as the Bejan number and porosity increase. Also, Figures 10–12 display curves of the optimal design variable behaviors against the applied Bejan number and porosity. In Figure 10, the optimal inlet and outlet diameters decrease as the Bejan number increases. There is a distinctive optimal configuration for given Bejan numbers that minimizes the wall peak temperature. Figures 11 and 12 depict the behavior of optimal channel diameter ratio $(d_{in}/d_{out})_{opt}$ and optimized channel-to-channel spacing ratio $(s_1/s_2)_{opt}$. The two variables are insensitive to the cooling enhancement, irrespective of the Bejan number and porosity. Their values approach unity for different Bejan numbers. These show that the inlet diameter and outlet diameter are almost equal, and the configuration approaches that of constant cross-section. Also, the $(s_1/s_2)_{opt}$ constant ratio can be seen as the values that will take care of the allowable wall thickness between the channels due to manufacturing constraints. These are adequate for the entire system to cool effectively.³⁸

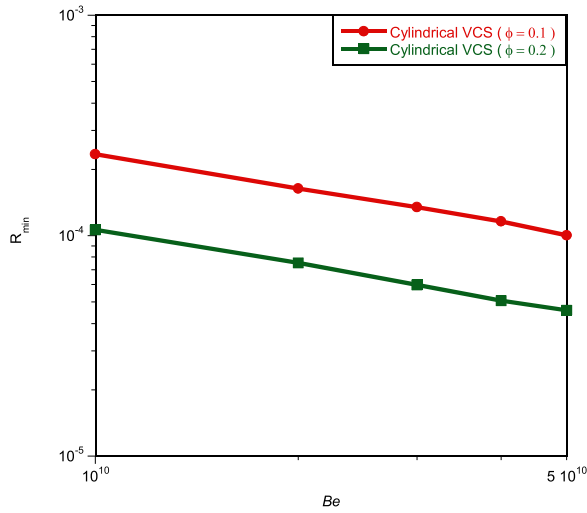


FIGURE 9 Effect of Bejan number on the minimized thermal resistance [Color figure can be viewed at wileyonlinelibrary.com]

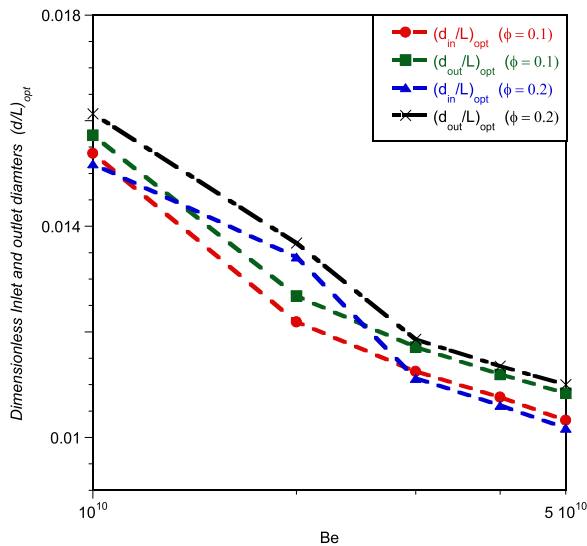


FIGURE 10 Effect of Bejan number on the optimized channel diameters, d_{in} and d_{out} [Color figure can be viewed at wileyonlinelibrary.com]

5.3 | Friction factor and pumping power calculations

The second objective function considered here is the minimized friction factor (f_{min}). This is numerically investigated for different Bejan numbers and porosities to evaluate its influence on the heat transfer fluid using Equation (18):

$$f_{min} = \frac{\pi^2 \rho \Delta P (d_{in})_{opt}^5}{8 \dot{m}^2 L} \tag{18}$$

where \dot{m} is the mass flow rate

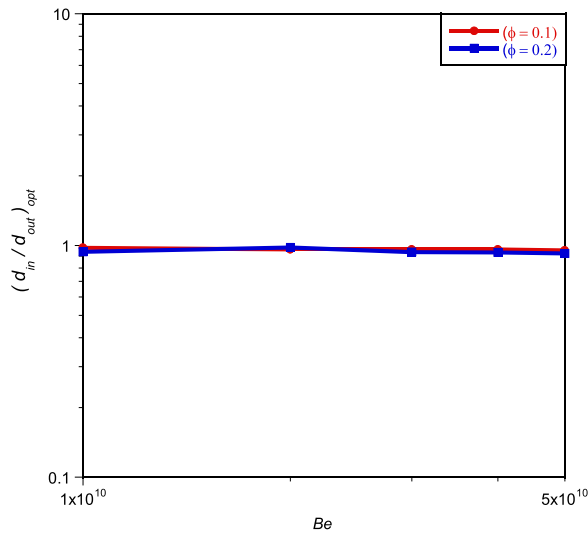


FIGURE 11 Effect of Bejan number on the optimized inlet and outlet diameters ratio [Color figure can be viewed at wileyonlinelibrary.com]

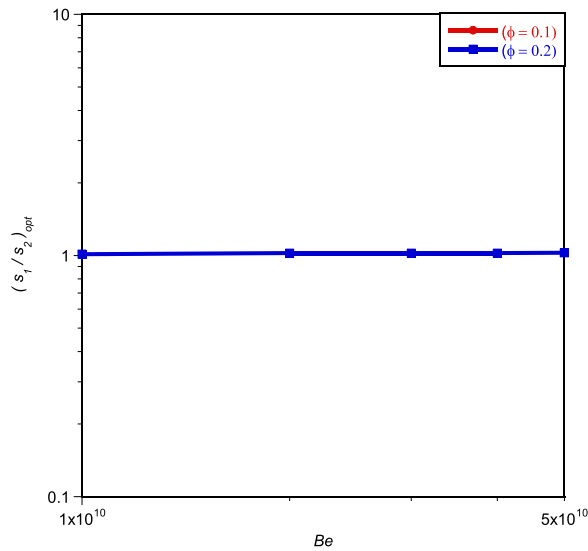


FIGURE 12 Effect of Bejan number on the optimized channel-to-channel spacing ratio [Color figure can be viewed at wileyonlinelibrary.com]

Figure 13 represents the effect of Bejan number on the friction factors. It shows that the minimized friction factor decreases as the Bejan number increases at given porosities. Also, when comparing Figures 9 and 13, it is observed that the decrease in minimized global thermal resistance is much higher than the decrease in the minimized friction factor as porosity and Bejan number increase. This behavior shows that the working fluid is efficient and effective for the entire cooling system.

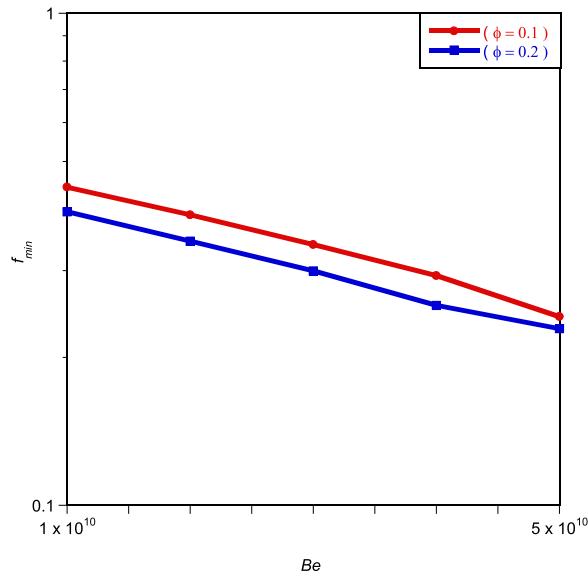


FIGURE 13 Effect of Bejan number on the minimized friction factors [Color figure can be viewed at wileyonlinelibrary.com]

Also, the required pumping power, which is characterized by energy consumption in evaluating the performance of the cooling channel, is calculated as follows:

$$(\text{Power})_{\text{Pump}} = \dot{V} \Delta P \tag{19}$$

where \dot{V} is the volumetric flow rate.

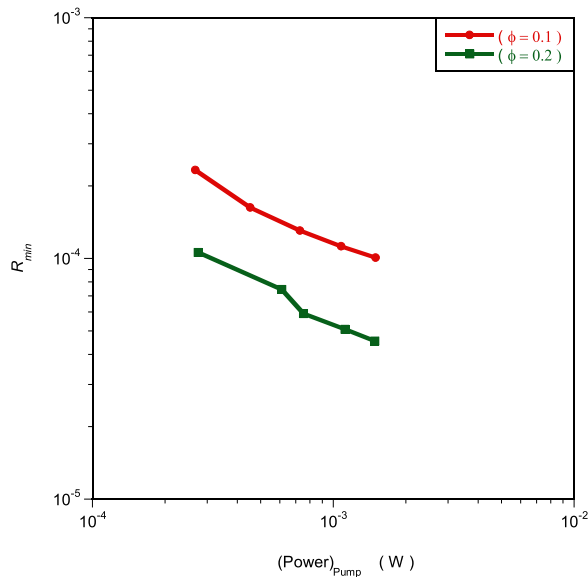


FIGURE 14 Effect of Pumping Power on the minimized thermal resistance [Color figure can be viewed at wileyonlinelibrary.com]

Figure 14 shows the influence of pumping power on thermal resistance at different porosities. It is important to know that pumping power and thermal resistance compete with each other: as the pumping power increases, minimized thermal resistance decreases significantly. This leads to a greater pressure drop and flow rate. The heat transfer enhancement is important, but higher pressure drop across the channel increases undesirably, leading to pumping power increment and higher energy consumption.

5.4 | Nusselt number calculation

Another important criterion considered in this study for thermal performance evaluation is the average Nusselt number (Nu), which characterizes the improvement of heat transfer. The maximized average Nusselt number is expressed as follows:

$$Nu_{\max} = \frac{h(d_{\text{in}})_{\text{opt}}}{k_f} \quad (20)$$

where h is average heat transfer coefficient expressed as follows:

$$h = \frac{\dot{q}_s''' L}{(T_w - T_{\text{in}})} \quad (21)$$

and T_w is the area-weighted average wall temperature.

Figure 15 shows the graph of the average Nusselt number against the Bejan number at different porosities. As the Bejan number and porosity increase, the average Nusselt number is maximized. Although the maximized average Nusselt increases as the Bejan number and porosity increase, it may not necessarily correspond to the best performance of the system. From the perspective of microelectronic cooling, it is essential to keep the maximum wall

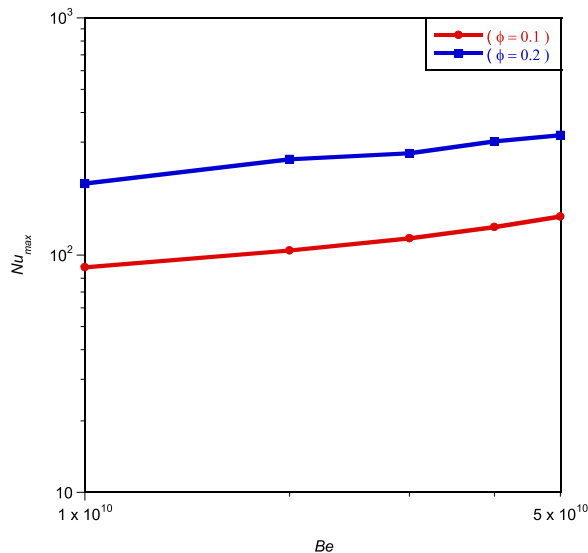


FIGURE 15 Effect of Bejan number on the maximized average Nusselt numbers [Color figure can be viewed at wileyonlinelibrary.com]

temperature less than the temperature specified by the manufacturers. This is why the thermal resistance that accounts for maximum wall temperature is used as the criterion to evaluate the best thermal and fluid flow performance of the system.

6 | COMPARISON BETWEEN RESULTS OF VARIABLE CROSS-SECTION AND CONSTANT CROSS-SECTION COOLING CHANNEL

Figure 16 reveals the optimal performance of the variable cross-section and constant cross-section microchannel configurations at different Bejan numbers and porosities. The results indicate that the thermal performance of the channel with variable cross-section is slightly better than that of the constant cross-section system. The percentage decrease is roughly 2% for all applied Bejan numbers and porosities. This slight variation is significantly adequate for better cooling of the entire system.

7 | CONCLUSION

This paper applies constructal theory and design to present a numerical geometric optimization of an array of parallel cylindrical microchannels with the variable cross-sectional region. The heat transfer problem is a conjugate with internal heat generation within the solid structure. The influences of geometric parameters on heat transfer and fluid flow were comprehensively studied. The numerical results show that as applied Bejan number and porosity increase, the minimized global dimensionless thermal resistance and friction factor decrease, whereas maximized average Nusselt number increases. Hence, the performance of heat transfer and fluid flow of the system is enhanced. Also, there are unique optimal inlet ($1.018 \times 10^{-2} \leq (d_{in}/L)_{opt} \leq 1.5381 \times 10^{-2}$) and outlet ($1.0838 \times 10^{-2} \leq (d_{out}/L)_{opt} \leq 1.6134 \times 10^{-2}$) diameters of variable cross-section configurations for a given Bejan number and porosity that minimized global thermal resistance and friction factor.

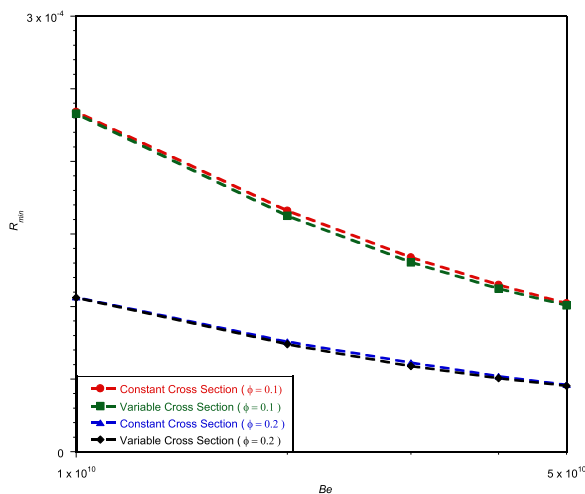


FIGURE 16 Comparison of optimal performance of constant cross-channel and variable cross-channel [Color figure can be viewed at wileyonlinelibrary.com]

The study reveals that the thermal performance is better when the channel inlet diameter is slightly less than that of the outlet diameter ($d_{in} < d_{out}$) for given Bejan number and porosity. The optimal channel diameter ratio $(d_{in}/d_{out})_{opt}$ and optimal channel-to-channel spacing ratio $(s_1/s_2)_{opt}$ remain constant as they approach unity value for different Bejan number. This means they are not sensitive to the system performance, irrespective of the Bejan number. These constant values of unity obtained could be described as the values that accounted for the allowable wall thickness between the channels due to industrial constraints and these are adequate for efficient cooling of the overall system.

Again, it is observed that the decrease in minimized global thermal resistance is much higher than the decrease in the minimized friction factor as Bejan number and porosity increase. This behavior indicates that the working fluid is efficient and effective for the entire cooling system.

The study demonstrates that the pumping power and thermal resistance compete with each other; as the pumping power increases, minimized thermal resistance decreases significantly. This leads to a greater pressure drop and flow rate, resulting in higher energy consumption. Moreover, the work shows that the maximized average Nusselt increases as the Bejan number and porosity increase. This increase in maximized average Nusselt may not necessarily correspond to the best performance of the system from the perspective of microelectronic cooling due to the fact that it is essential to keep the maximum wall temperature less than the temperature specified by the manufacturers. This is why the thermal resistance that accounts for maximum wall temperature is used as the criterion to evaluate the best thermal and fluid flow performance of the system.

Also, the study reveals that the optimal performance of the variable cross-sectional cooling channel configuration is slightly better than that of the constant cross-sectional cooling channel configuration by 2% for applied Bejan numbers at different porosities. This percentage variation in thermal resistance is significant and enough for efficient cooling of the entire system.

ACKNOWLEDGMENT

The support received from the University of Lagos is acknowledged and appreciated.

DATA AVAILABILITY STATEMENT

Data sharing is not applicable to this article, as no datasets were generated or analyzed during the current study.

NOMENCLATURE

A_{ch}	cross-sectional area of the channel (m^2)
A_s	cross-sectional area of the structure (m^2)
Be	Bejan number
C_p	specific heat at constant pressure ($J\ kg\ J$)
CCS	constant cross-section
d_h	hydraulic diameter (m)
f	fluid
f	friction factor
h	elemental height (m)
h	coefficient of heat transfer ($W/m^2\ K$)
H	structure height (m)
i	mesh iteration index

In	inlet
K	thermal conductivity (W/mK)
L	axial length (m)
max	maximum peak
min	minimum
N	normal
Nu	average Nusselt number
Opt	optimum
Out	outlet
P	pressure (Pa)
P_r	Prandtl number
q	heat transfer rate (W)
\dot{q}''	heat flux (W/m ²)
\dot{q}'''_s	internal heat generation (W/m ³)
R	thermal resistance
Re	Reynolds number
s	channel–channel spacing (m)
T	temperature (°C)
\vec{v}	velocity vector (m/s)
v_{ch}	channel volume (m ³)
v_{el}	elemental volume (m ³)
V_s	global structure volume (m ³)
VCS	variable cross-section
w	structure width (m)
w	elemental width (m)
w	wall
x, y, z	cartesian coordinates (m)
α	thermal diffusivity (m ² /s)
μ	viscosity (kg/m s)
s	solid
ρ	density (kg/m ³)
∂	differential
ϕ	porosity
Δ	difference
∇	differential operator
γ	convergence criterion

ORCID

Olabode T. Olakoyejo  <http://orcid.org/0000-0001-9942-1339>

Adekunle O. Adelaja  <http://orcid.org/0000-0001-9175-8332>

Saheed A. Adio  <http://orcid.org/0000-0002-2732-1360>

REFERENCES

1. Bejan A. *Advanced Engineering Thermodynamics*. 2nd ed. New York, NY: Wiley; 1997.
2. Bejan A. *Shape and Structure from Engineering to Nature*. Cambridge: Cambridge University Press; 2000.
3. Bejan A, Lorente S. *Design with Constructal Theory*. Hoboken, NJ: John Wiley; 2008.

4. Bejan A. *The Physics of Life: the Evolution of Everything*. New York, NY: St. Martins Press; 2016.
5. Mustafa AW. Constructral design of multi-scale diamond-shaped pin fins cooled by mixed convection. *Int J Thermal Sci*. 2019;145:106018.
6. Miguel AF, Rocha LAO. *Tree-Shaped Fluid Flow and Heat Transfer*. New York, NY: Springer; 2018.
7. Bejan A. Constructral law, twenty years after. *Proc Romanian Acad Series A, Math Phys Tech Sci Inform Sci*. 2018;18:309-311.
8. Chen LG, Feng HJ, Xie ZH, Sun FR. Progress of constructral theory in China over the past decade. *Int J Heat Mass Transfer*. 2019;130:393-419.
9. Lorente S, Bejan A. Current trends in constructral law and evolutionary design. *Heat Transfer-Asian Res*. 2019;48:57-389.
10. Bejan A. *Freedom and Evolution: Hierarchy in Nature, Society and Science*. Springer; 2020.
11. Chen LG, Yang AB, Feng HJ, Ge YL, Xia SJ. Constructral designs for eight types of heat sinks. *Sci China: Technol Sci*. 2020;63:879-911.
12. You J, Feng HJ, Chen LG, Xie ZH, Xia SJ. Constructral design and experimental validation of a non-uniform heat generating body with rectangular cross-section and parallel circular cooling channels. *Int J Heat Mass Transfer*. 2020;148:119028.
13. Feng HJ, Cai CG, Chen LG, Wu ZX, Lorenzini G. Constructral design of a shell-and-tube condenser with ammonia-water working fluid. *Int Comm Heat Mass Transfer*. 2020;118:104867.
14. Mustafa AW. Maximization of heat transfer density rate from a single row of rhombic tubes cooled by forced convection based on constructral design. *Heat Transfer-Asian Res*. 2019;48:624-643.
15. Mustafa AW, Ghani IA. Maximization of heat transfer density from a vertical array of flat tubes in cross flow under fixed pressure drop using constructral design. *Heat Transfer-Asian Res*. 2019;48:3489-3507.
16. Gupta A, Singh H. Optimum design study of a straight tube with different inserts for thermal performance characteristics. *Heat Transfer*. 2020;49:1955-1981.
17. Bello-Ochende T, Olakoyejo OT, Meyer JP. Constructral flow orientation in conjugate cooling channels with internal heat generation. *Int J Heat Mass Transfer*. 2013;57:2411-249.
18. Qu W, Mudawar I. Analysis of three-dimensional heat transfer in micro-channel heat sinks. *Int J Heat Mass Transfer*. 2002;45:3973-3985.
19. Jia Y, Xia G, Li Y, Ma D, Cai B. Heat transfer and fluid flow characteristics of combined microchannel with cone-shaped micro pin fins. *Int Com Heat Mass Transfer*. 2018;92:78-89.
20. Bejan A, Sciubba E. The optimal spacing of parallel plates cooled by forced convection. *Int J Heat Mass Transfer*. 1992;35:3259-3264.
21. Bejan A, Badescu V, de Vos A. Constructral theory of economics. *Appl Energy*. 2000;67:37-60.
22. Bejan A. Optimal internal structure of volumes cooled by single phase forced and natural convection. *J Electron Packaging*. 2003;125:200-207.
23. Bejan A. Two hierarchies in science: the free flow of ideas and the academy. *Int J Design Nature Ecodyn*. 2009;4:386-394.
24. Reis AH, Miguel AF, Aydin M. Constructral theory of flow architecture of the lungs. *Med Phys*. 2004;31:1135-1140.
25. Rocha LOA, Lorenzini E, Biserni C. Geometric optimization of shapes on the basis of Bejan's Constructral theory. *Int Comm Heat Mass Transfer*. 2005;32:1281-1288.
26. Salimpour MR, Sharifhasan M, Shirani E. Constructral optimization of the geometry of an array of micro-channels. *Int Comm Heat Mass Transfer*. 2010;38(2010):93-99.
27. Olakoyejo OT, Bello-Ochende T, Meyer JP. Mathematical optimisation of laminar forced convection heat transfer through a vascularised solid with square channels. *Int J Heat Mass Transfer*. 2012;55:2402-2411.
28. Bello-Ochende T, Liebenberg L, Meyer JP. Constructral cooling channels for micro-channel heat sinks. *Int J Heat Mass Transfer*. 2007;50(21-22):4141-4150.
29. Bello-Ochende T, Meyer JP, Ighalo FU. Combined numerical optimization and constructral theory for the design of micro-channel heat sinks. *Numer Heat Transfer, Part A*. 2010;58:882-899.
30. Adewumi OO, Bello-Ochende T, Meyer JP. Constructral design of combined microchannel and micro pin fins for electronic cooling. *Int J Heat Mass Transfer*. 2013;66:315-323.
31. Yilmaz A, Buyukalaca O, Yilmaz T. Optimum shape and dimensions of ducts for convective heat transfer in laminar flow at constant wall temperature. *Int J Heat Mass Transfer*. 2000;43:767-775.

32. Rocha LAO, Lorenzini E, Biserni C, Cho Y. Constructal design of a cavity cooled by convection. *Int J Des Ecodyn*. 2010;5:212-220.
33. Biserni C, Rocha LAO, Stanescu G, Lorenzini E. Constructal H-shaped cavities according to Bejan's theory. *Int J Heat Mass Transfer*. 2007;50:2132-2138.
34. Lorenzini G, Biserni C, Isoldi LA, Dos Santos ED, Rocha LAO. Constructal design applied to the geometric optimization of Y-shaped cavities embedded in a conducting medium. *J Electron Packaging Trans ASME*. 2011;133:041008.
35. Lorenzini G, Biserni C, Estrada ED, Isoldi LA, dos Santos ED, Rocha LAO. Constructal design of convective Y-shaped cavities by means of genetic algorithm. *ASME J Heat Transfer*. 2014;136:071702.
36. Muzychka YS. Constructal multi-scale design of compact micro-tube heat sinks and heat exchangers. *Int J Thermal Sci*. 2007;46:245-252.
37. Xie G, Shen H, Wang CC. Parametric study on thermal performance of microchannel heat sinks with internal vertical Y-shaped bifurcations. *Int J Heat Mass Transfer*. 2015;90:948-958.
38. Olakoyejo OT, Bello-Ochende T, Meyer JP. Constructal conjugate cooling channels with internal heat generation. *Int J Heat Mass Transfer*. 2012;55:4385-4396.
39. Meyer JP, Olakoyejo OT, Bello-Ochende T. Constructal optimisation of conjugate triangular cooling channels with internal heat generation. *Int Com Heat Mass Transfer*. 2012;39:1093-1100.
40. Olakoyejo OT. Geometric optimisation of conjugate heat transfer in cooling channels with different cross-sectional shapes (PhD Thesis). Department of Mechanical and Aeronautical Engineering, University of Pretoria; 2012.
41. Bhattacharjee S, Grosshandler WL. The formation of wall jet near a high temperature wall under micro-gravity environment. *ASME HTD*. 1998;96:711-716.
42. Petrescu S. Comments on the optimal spacing of parallel plates cooled by forced convection. *Int J Heat Mass Transfer*. 1994;37(994):1283.
43. Awad MM. The science and the history of the two Bejan numbers. *Int J Heat Mass Transf*. 2016;94:101-103.
44. Rickard RF, Meyer C, Hudson DA. Computational modeling of microarterial anastomoses with size discrepancy (small-to-large). *J Surg Res*. 2009;153:1-11. <https://www.fluent.com>
45. Patankar SV. *Numerical Heat Transfer and Fluid flow*. Hemisphere, NY: CRC Press; 1980.
46. White FM. *Viscous Fluid Flow*. 2nd ed. Singapore: McGraw-Hill; 1991.
47. Myers RH, Montgomery DC. *Response Surface Methodology: Process And Product Optimization Using Designed Experiment*. New York, NY: Wiley; 2002.
48. Aduralere TT, Olakoyejo OT, Adewumi OO, Adelaja AO, Obayopo SO, Meyer JP. Numerical optimisation of forced convection of wall thickness of heated plates cooled using aluminawater nanofluid. In: *Proceedings of the 16th International Heat Transfer Conference*, Beijing, China; 2018:2969-2976.

How to cite this article: Olakoyejo OT, Adelaja AO, Adewumi OO, Oluwo AA, Bello SK, Adio SA. Constructal heat transfer and fluid flow enhancement optimization for cylindrical microcooling channels with variable cross-section. *Heat Transfer*. 2021;1-19. <https://doi.org/10.1002/htj.22202>